

ARTICLE

Received 23 Jun 2014 | Accepted 29 Sep 2014 | Published 10 Nov 2014

DOI: 10.1038/ncomms6407

OPEN

Progressive contraction of the latent HIV reservoir around a core of less-differentiated CD4⁺ memory T Cells

S. Jaafoura^{1,*}, M.G. de Goër de Herve^{1,*}, E.A. Hernandez-Vargas², H. Hendel-Chavez¹, M. Abdoh¹, M.C. Mateo¹, R. Krzysiek^{3,4}, M. Merad⁵, R. Seng⁶, M. Tardieu^{1,4}, J.F. Delfraissy^{1,4,7}, C. Goujard^{4,5,7} & Y. Taoufik^{1,4}

In patients who are receiving prolonged antiretroviral treatment (ART), HIV can persist within a small pool of long-lived resting memory CD4⁺ T cells infected with integrated latent virus. This latent reservoir involves distinct memory subsets. Here we provide results that suggest a progressive reduction of the size of the blood latent reservoir around a core of less-differentiated memory subsets (central memory and stem cell-like memory (T_{SCM}) CD4⁺ T cells). This process appears to be driven by the differences in initial sizes and decay rates between latently infected memory subsets. Our results also suggest an extreme stability of the T_{SCM} sub-reservoir, the size of which is directly related to cumulative plasma virus exposure before the onset of ART, stressing the importance of early initiation of effective ART. The presence of these intrinsic dynamics within the latent reservoir may have implications for the design of optimal HIV therapeutic purging strategies.

¹INSERM U1012, 94276 Le Kremlin-Bicêtre, France. ²Systems Medicine of Infectious Diseases, Helmholtz Centre for Infection Research, Inhoffenstraße 7, 38124 Braunschweig, Germany. ³INSERM U996, 92140 Clamart, France. ⁴Faculté de Médecine, Université Paris-Sud, 94276 Le Kremlin-Bicêtre, France. ⁵Department of Medicine, Institut Gustave Roussy, 94805 Villejuif, France. ⁶INSERM U1018, 94275 Le Kremlin-Bicêtre, France. ⁷Department of Internal Medicine, Hôpitaux Universitaires Paris-Sud, 94275 Le Kremlin-Bicêtre, France. * These authors contributed equally to this work. Correspondence and requests for materials should be addressed to Y.T. (email: yassine.taoufik@bct.aphp.fr).

Although combined antiretroviral therapy (ART) generally suppresses HIV replication to undetectable plasma levels for prolonged periods, it fails to eradicate the virus. HIV can persist within a small pool of long-lived resting memory CD4⁺ T cells infected with integrated latent virus^{1–4}. This latent reservoir appears to involve several memory CD4⁺ T-cell subsets at distinct differentiation stages with different phenotypic and functional properties, forming distinct ‘sub-reservoirs’^{5,6}. Precise immunological characterization of the latent CD4⁺ T-cell reservoir, including the size of each sub-reservoir, is crucially important for the complex challenge of ‘therapeutic purging’. The relative size of each sub-reservoir may depend on its decay rate and may therefore vary according to the time on ART.

Here we show the existence of a dynamic process that progressively reduces the size of the latent reservoir around a core of less differentiated memory CD4 T-cell subsets (for example, central memory CD4⁺ T cells and the recently identified stem cell-like memory CD4⁺ T cells). Our results also stress the importance of early initiation of effective ART to limit the size of the T_{SCM} sub-reservoir, which appears directly related to cumulative plasma virus exposure.

Results

Study design. We examined the decay rates of resting memory subsets latently infected by HIV in highly selected patients with consistently undetectable plasma virus on ART. Cell sorting of CD4⁺ T-cell memory subsets requires the use of fresh peripheral blood mononuclear cells (PBMC), as cryopreservation alters the expression of markers, such as CD62L, which is required to sort the different memory subsets^{7,8} (see also Supplementary Fig. 1). This ruled out a retrospective study on frozen cells. Furthermore, a longitudinal prospective study can take more than a decade. We therefore chose to conduct a cross-sectional analysis on strictly selected patients from a cohort of 360 HIV-1-infected patients (see methods). The characteristics of patients who fulfilled the selection criteria and were enrolled are shown in Supplementary Table 1. The recently identified T_{SCM} subset consists of rare CD4⁺ memory T cells with stem cell-like features⁹. In response to recall antigens, T_{SCM} exhibited the strongest proliferation among the tested memory cell subsets (Supplementary Fig. 2). Figure 1a shows the gating strategy used to sort highly purified resting T_{SCM} (see also Supplementary Fig. 3 for purity). Resting central memory (T_{CM}) and effector memory CD4⁺ T cells (T_{EM}) were sorted on the basis of stringent criteria⁹. An additional resting CD4⁺ T-cell memory subset with an intermediate CCR7⁻ CD62L⁺ phenotype, designated T_{IM} (intermediate memory), was also sorted (see Methods). Infectious virus was recovered from the four resting memory cell subsets following *in vitro* activation (see Supplementary Fig. 4).

Tight homeostatic regulation of T_{SCM}. Cell numbers of the different memory subsets per mm³ of blood were similar in the patients with undetectable plasma virus and in a group of HIV-seronegative healthy donors (Fig. 1b). In contrast, in a group of patients with chronic active viral replication, the T_{SCM} and T_{CM} CD4⁺ subsets were significantly depleted (Fig. 1b). Within the pool of memory CD4⁺ T cells, the distribution of the different memory subsets was markedly different between patients with chronic active HIV replication and HIV-seronegative donors (Fig. 1c). This was mainly due to a significant increase in the proportions of T_{EM} and T_{IM}, to the detriment of T_{CM} ($P < 0.01$ each for the percentages of T_{CM}, T_{EM} and T_{IM} within the pool of memory CD4⁺ T cells; Kruskal–Wallis and Dunn’s tests; see Supplementary Fig. 5). Possible explanations for these differences include increased differentiation of T_{CM} towards memory effector

subsets, higher susceptibility of T_{CM} to infection-induced cell death and altered T_{CM} trafficking between secondary lymphoid tissues and blood. In the patients with undetectable plasma virus on ART, the percentages of T_{CM} and T_{EM} within the pool of memory CD4⁺ T cells were significantly different when compared with healthy donors ($P < 0.01$; Kruskal–Wallis and Dunn’s tests), but were not different when compared with patients with active virus replication (see Supplementary Fig. 5). The percentage of T_{IM} was not different between patients on ART with undetectable virus and both healthy donors and viremic patients. As shown in Fig. 1c, the distribution of the different subsets within memory CD4⁺ T cells differed between the patients with undetectable plasma virus on ART and both the patients with active virus replication and the healthy donors. This suggested that recovery of the CD4⁺ T-cell memory pool during prolonged effective ART was incomplete. Interestingly, there was no significant difference in the percentage of T_{SCM} within memory CD4⁺ T cells between the patients on prolonged effective ART, the patients with active virus replication and the healthy donors (see Supplementary Fig. 5). This suggests tight homeostatic regulation maintaining the equilibrium between T_{SCM} and the rest of the memory CD4⁺ T cells despite active virus replication. In each group of patients and healthy donors analysed, there was no significant relation between the age and the absolute numbers of T_{SCM} per mm³ of blood ($P = 0.12$, 0.53 and 0.69, for patients with chronic active virus replication, patients on prolonged effective ART and healthy donors, respectively, Spearman Rank Test) or the percentage of T_{SCM} within memory CD4⁺ T cell ($P = 0.83$, 0.11 and 0.11, respectively, Spearman Rank Test).

A highly stable Core of latently infected T_{SCM} and T_{CM}. Integrated HIV DNA was quantified in sorted CD4 memory subsets with a well-established Alu-gag PCR method^{10,11} (see Methods and Supplementary Fig. 6). Sorted naive CD4⁺ T cells (CD45RA⁺ CD45RO⁻ CCR7⁺ CD62L⁺ CD27⁺ CD95⁻) were also tested, but in our series integrated HIV DNA was detected in truly naive cells only in 18.4% of patients (see Supplementary Fig. 7). The results obtained for memory subsets are shown in Fig. 2a. The best linear regression of our data suggested that the T_{SCM} sub-reservoir had the longest half-life among the latently infected memory subsets analysed (not shown). However, to take possible inter-patient variability into account and to validate this cross-sectional analysis, the results were analysed with the Monte Carlo (MC) algorithm (see Methods). Briefly, we performed 10⁶ computer simulations with random samplings for each latently infected memory subset, based on the mean values and variance of our experimental data. For each simulation, we fitted the number of integrated HIV DNA copies per 10⁵ cells at the time of undetectable plasma virus following ART initiation (y_0) and the slope of decay (λ). The mean values of y_0 and λ obtained from the 10⁶ simulations were used to plot the decay curves shown in Fig. 2a. The distribution of y_0 and λ for each latently infected memory subset is indicated in Supplementary Fig. 8. The mean value of λ was used to estimate the half-life ($-\ln 2/\lambda$) of each latent sub-reservoir. The mean y_0 , λ and half-life values were as follows: 16.54 integrated copies per 10⁵ cells, $-0.0025 \text{ month}^{-1}$ and 277 months for T_{SCM}; 55.54 integrated copies per 10⁵ cells, $-0.0048 \text{ month}^{-1}$ and 144 months for T_{CM}; 42.92 integrated copies per 10⁵ cells, $-0.0052 \text{ month}^{-1}$ and 133 months for T_{IM} and 59.88 integrated copies per 10⁵ cells, $-0.0079 \text{ month}^{-1}$ and 88 months for T_{EM}. Analysis of the MC results (two-way analysis of variance and *t*-test (significance at $P < 0.05$), with a Bonferroni post-test) confirmed that the T_{SCM} latent reservoir had a slower decay rate

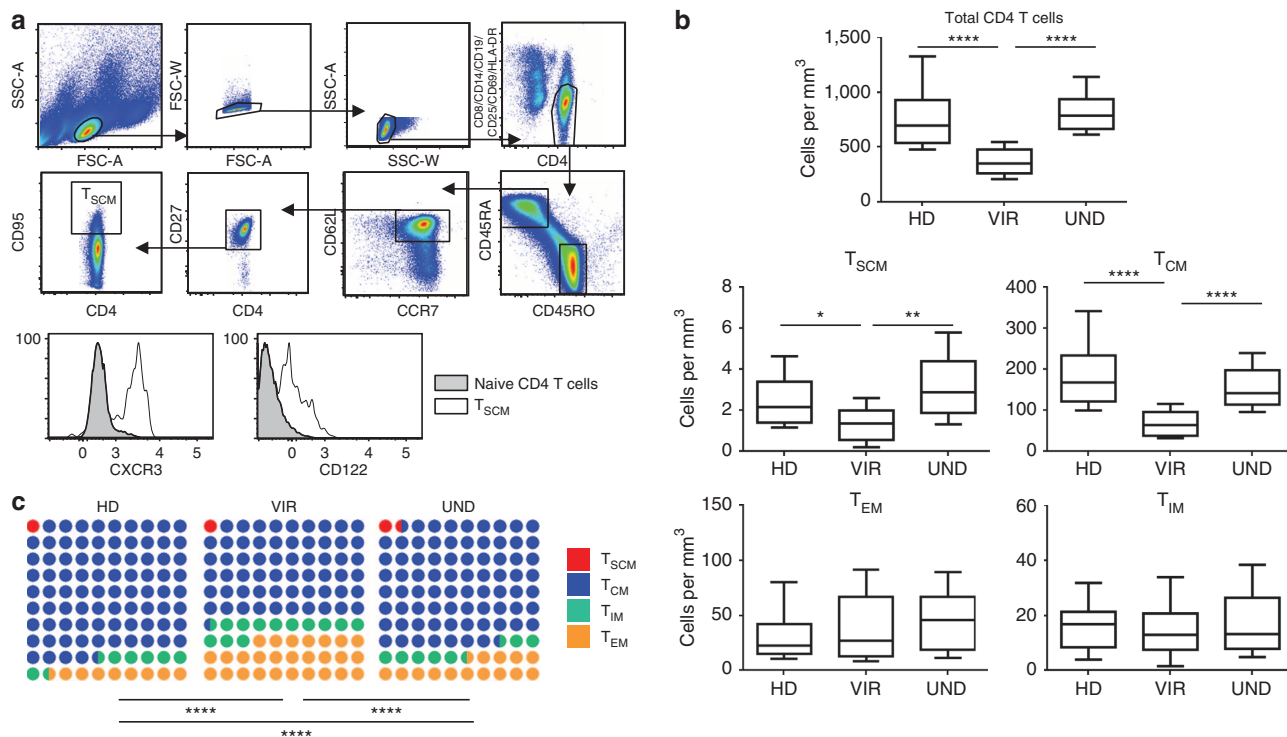


Figure 1 | During HIV infection the relative size of the T_{SCM} subset within memory CD4 T cells remains stable. (a) The gating strategy used to sort the memory cell subsets: CD4-enriched PBMC were stained with a cocktail of antibodies (see Methods) and doublets were excluded on the basis of both forward scatter (FSC) and side scatter (SSC). Resting CD4⁺ T cells were gated after exclusion of CD19⁺, CD14⁺, CD8⁺, HLADR⁺, CD69⁺, CD25⁺ cells. Resting T_{SCM} were sorted on the basis of the following phenotype: CD45RA⁺ CD45RO⁻ CCR7⁺ CD62L⁺ CD27⁺ CD95⁺. CXCR3 and CD122 expression by T_{SCM} is also shown. (b) The absolute number of cells in each memory subset (T_{SCM} , T_{CM} , T_{EM} and T_{IM}) was determined in HIV-infected patients with undetectable plasma viral load on ART and with CD4 cell counts above 500 per mm³, who were tested for integrated virus (UND, *n* = 38), as well as in age- and sex-matched viremic patients (VIR, *n* = 18) and HIV-seronegative healthy donors (HD, *n* = 20). The Kruskal-Wallis and Dunn tests were used for statistical analysis (**P* < 0.05, ***P* < 0.01, *****P* < 0.0001). Boxes represent the median and the 25th and 75th percentiles; whiskers represent the 10th and 90th percentiles. (c) Shows the percentage of each memory subset within the compartment formed by the four memory subsets analysed. The χ^2 test was used to analyse differences in the distribution of the four memory subsets (*****P* < 0.0001).

than the other studied sub-reservoirs (*P* < 0.05), whereas no significant difference was found between the decay rates of T_{CM} , T_{IM} and T_{EM} (see also Supplementary Fig. 8a). The same analysis also showed that T_{SCM} had a lower number of integrated copies than the other sub-reservoirs at the time of undetectable plasma virus following ART initiation (y_0 ; *P* < 0.05), whereas no significant difference was found between T_{CM} , T_{IM} and T_{EM} (see also Supplementary Fig. 8b).

We then predicted the individual decay of each latently infected memory subset within the entire blood volume (Fig. 2b), as well as long-term changes in the relative proportions of the different memory subsets forming the latent CD4⁺ T-cell reservoir (Fig. 2c). For this purpose, we took into account the y_0 and decay rate values of each sub-reservoir obtained by MC analysis, together with the absolute number of cells composing each CD4⁺ memory subset in the entire blood volume (see Methods and legend to Fig. 2b,c). We found the following hierarchy in the total sizes of the different memory sub-reservoirs in the entire blood volume at the time of undetectable plasma virus following ART initiation: $T_{CM} > T_{EM} > T_{IM} > T_{SCM}$ (*P* > 0.05; Fig. 2b). The relative size of the T_{SCM} sub-reservoir within the latent memory reservoir then increased over time, owing to the longer half-life of these cells (Fig. 2b,c). The data predicted that the size difference between T_{SCM} , T_{EM} and T_{IM} sub-reservoirs would become non-significant after 50 years on effective ART, whereas the T_{CM} sub-reservoir would remain larger than the other three sub-reservoirs (Fig. 2b). The decay of

the whole-blood latent CD4⁺ T-cell memory reservoir appeared to be driven mainly by the decay rate of the T_{CM} sub-reservoir (Fig. 2b). The results also imply that it would take more than 100 years for T_{EM} , the most labile latent sub-reservoir, to be eradicated by ART, without additional therapeutic approach (Fig. 2b). Altogether, T_{SCM} and T_{CM} appear to form the most stable part of the latent CD4⁺ T-cell memory reservoir, mainly owing to the extremely long half-life of T_{SCM} and to the larger size of the T_{CM} reservoir at the initiation of effective ART (Fig. 2b,c).

T_{SCM} reservoir size is related to cumulative HIV exposure.

We then examined the influence of several parameters on the frequency of integrated HIV in each memory CD4⁺ T-cell subset at the time when plasma virus became undetectable (see legend of Fig. 3), including age and sex, the CD4⁺ T-cell nadir, the duration of detectable HIV viremia and cumulative HIV plasma viremia. Cumulative plasma viremia, expressed in log₁₀ virus copy-years, is a measure of cumulative plasma viral load exposure during a given time period¹². As shown in Fig. 3a–c, the frequency of integrated HIV DNA in T_{SCM} correlated positively with cumulative HIV plasma viremia, over a period up to 7 years before plasma virus becoming undetectable, whereas no such relation was found for the other memory subsets (Fig. 3b,c). None of the other parameters significantly influenced the size of the latently infected memory subsets (*P* values ranged to from

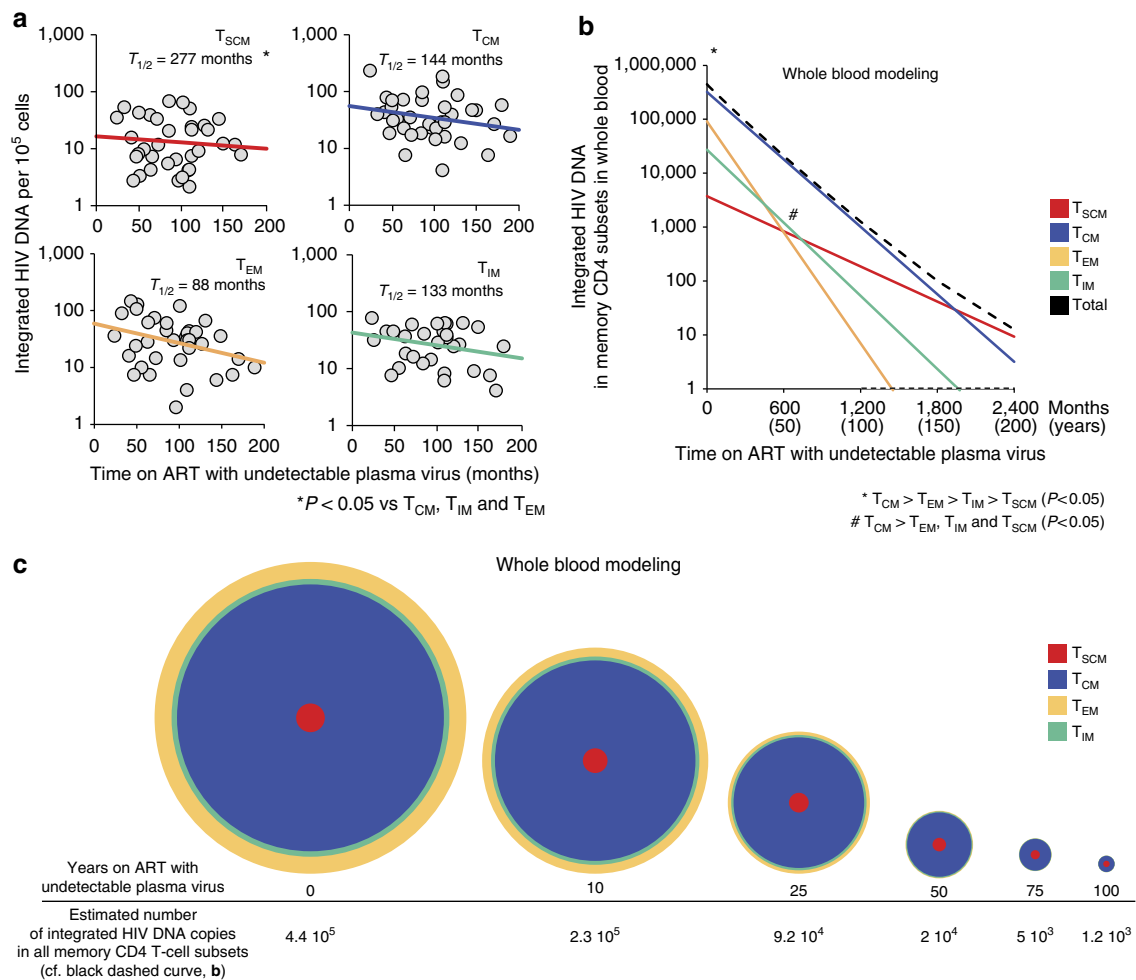


Figure 2 | Slow reduction of the latent HIV reservoir around a core formed mainly by T_{SCM} and T_{CM} . (a) Integrated HIV DNA was quantified in T_{SCM} , T_{CM} , T_{EM} and T_{IM} isolated from 38 strictly selected patients in whom viral load was undetectable for 24–189 months on ART. Recovery of T_{EM} and T_{SCM} was suboptimal in three patients. T_{IM} could not be isolated from nine patients. The results are expressed as the integrated HIV DNA copy number per 10^5 cells. Taking inter-patient variability into account, the data shown in a were analysed with the Monte Carlo algorithm with 10^6 computer simulations with random samplings for each latently infected memory subset (see Methods). For each simulation, the number of integrated HIV DNA copies per 10^5 cells at the time of undetectable plasma virus following ART initiation (y_0) and the slope of decay (λ) were fitted. The distributions of y_0 and λ obtained from the 10^6 simulations are shown in Supplementary Fig. 8. The mean values of y_0 and λ were used to plot the decay curves shown in a. The mean half-life of decay ($-\ln 2/\lambda$) is indicated for each latently infected memory subset. Statistical significance is indicated as * (for statistical analysis, see the Monte Carlo section of Methods). (b) Extends the data shown in a to the entire blood compartment. To analyse the decay in absolute numbers of latently infected memory subsets in the whole blood compartment, we used the 10^6 simulation values of y_0 and slopes of decay obtained for each memory subset following Monte Carlo analysis. The predictions shown in b correspond to the average values of y_0 and slopes. For the other parameters required to calculate the absolute numbers of latently infected cells (body weight, CD4 T-cell count and the percentages of the memory subsets among total CD4 T cells), we used the median values from our cohort of 38 patients. Total blood volume was estimated to represent 7% of total body weight²⁹. Note that the predictions in b remained consistent when random sampling (Monte Carlo approach) was used for body weight, the CD4⁺ T-cell count and the percentages of memory subsets among total CD4⁺ T cells, based on the median values and variance for the patients analysed. We considered 50 time points from 0 to 200 years (a total of 50×10^6 values for each memory subset). Comparison between the memory subsets was performed as in a. (See in Methods the Monte Carlo section). Statistical significance is indicated *, #. (c) The immunological dynamics of the CD4⁺ T-cell latent reservoir, corresponding to changes, at chosen time-points, in the relative size of each memory subset within the compartment formed by the four latently infected memory subsets in the entire blood compartment (see above). The surface areas are proportional to the numbers of integrated HIV DNA copies in each memory CD4 subset in the entire blood volume (predictions shown in b).

0.18–0.9, Spearman rank test). Together, the results suggested that the size of the T_{SCM} sub-reservoir is more directly influenced by the level and duration of plasma virus exposure than the other sub-reservoirs.

Discussion

Together, these results reveal the existence of an intrinsic dynamic process within the latent reservoir that contracts around

a core of less-differentiated memory subsets (T_{CM} and T_{SCM}). This slow process is driven by differences in initial sizes and decay rates of the latently infected memory subsets. The half-life of each latently infected subset may be related to the intrinsic capacity of its component cells to survive and to self-renew. Several lines of evidence suggest that homeostatic proliferation, including in response to IL-7, may not necessarily lead to efficient reactivation of latent HIV and subsequent cell destruction, thus allowing self-renewing cells and their progeny to persist in the latent CD4⁺

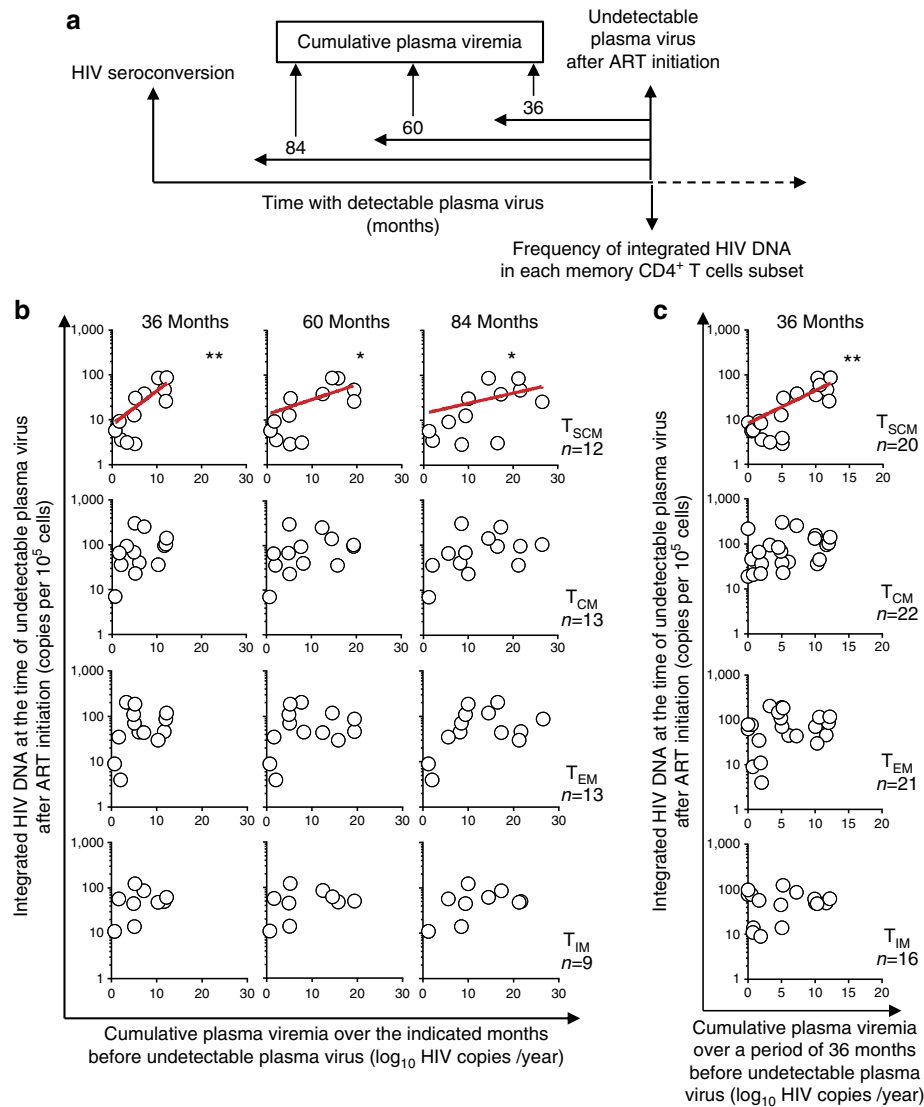


Figure 3 | The frequency of latent infection of T_{SCM} is related to cumulative plasma virus exposure. (a,b) Cumulative viremia, expressed as \log_{10} virus copy-years during periods of 36, 60 and 84 months before plasma virus became undetectable, was determined in patients ($n=9-13$) for whom virological follow-up was available for a period of 84 months. Associations were sought between cumulative viremia and the frequency of latent infection of each memory subset at the time when plasma virus became undetectable after ART initiation. For each patient, the frequency of latent infection of each memory subset at the time when plasma virus became undetectable after ART initiation was calculated from the slopes of the decay curves shown in Fig. 2a. The number of patients for whom virological follow-up was available over a period longer than 84 months before undetectable plasma virus, was insufficient for statistical analysis. In c, the same analysis was performed for all patients ($n=16-22$) for whom virological follow-up was available over a period of 36 months before plasma virus became undetectable. The Spearman rank test was used for statistical analysis (* $P < 0.05$, ** $P < 0.01$).

T-cell reservoir^{5,13,14}. Long-term survival and self-renewal are key properties of T_{SCM} and, to a lesser extent, of T_{CM} ⁹. These features may explain the greater stability of the T_{SCM} reservoir as compared with the more highly differentiated $CD4^+$ T-cell memory subsets. However, the half-lives of latently infected memory subsets may also be influenced by cell transfer from other compartments. For example, in response to homeostatic signals, T_{SCM} can generate more highly differentiated cells such as T_{CM} and T_{EM} while maintaining their own pool^{9,15}, thereby fueling downstream compartments.

A recent work suggested that T_{SCM} harbour the highest level of HIV DNA among memory T-cell subsets regardless of the time on ART, with a considerable inter-individual variations¹⁶. Our results do not support this finding. We found that the T_{SCM} sub-reservoir has great stability but at the time when plasma virus became undetectable on ART, it harbours the lowest level

of stable infection among latently infected memory subsets. Noteworthy, the authors used a PCR procedure that quantifies total HIV DNA including integrated and unintegrated labile virus. The latter may reflect residual virus expression^{17,18} that may increase inter-individual variability of total HIV DNA.

Why does cumulative plasma virus exposure influence the formation of the latent T_{SCM} sub-reservoir more strongly than the formation of other memory sub-reservoirs? One possibility is the existence of additional factors that influence the formation of latently infected $CD4^+$ T cells in addition to viral exposure and that are more active in T_{EM} , T_{IM} and T_{CM} . These might include immunological factors that negatively regulate cell activation, such as cell-surface inhibitory receptors. The level of PD-1 expression has been shown to influence the level of latent infection in $CD4$ T cells in patients on ART⁵. As shown in Fig. 4a,b, a lower PD-1 expression was found on T_{SCM} as

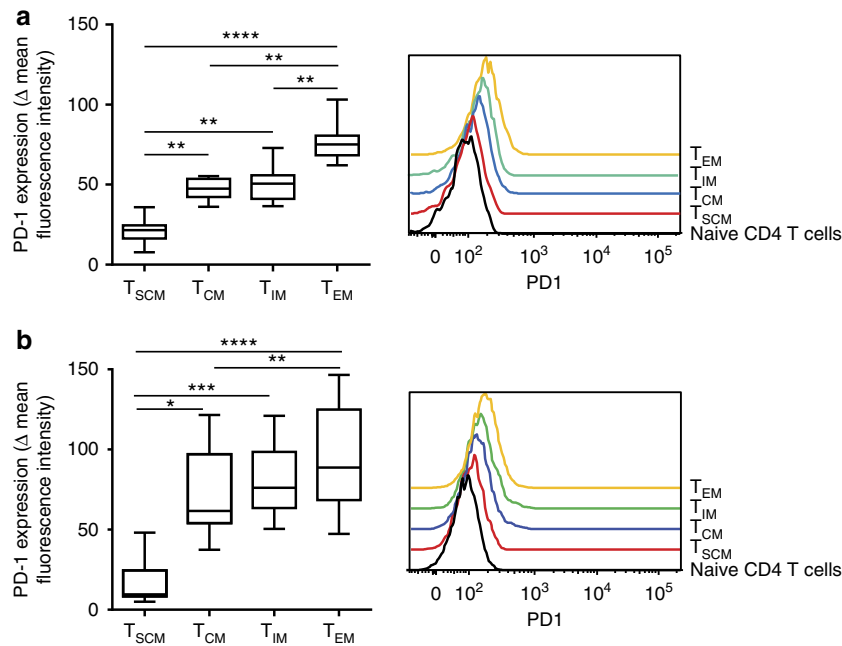


Figure 4 | PD-1 is less strongly expressed on T_{SCM}. Surface PD-1 expression on blood memory CD4⁺ T-cell subsets was analysed in 15 patients with CD4⁺ T-cell counts >500 per mm³ and undetectable plasma virus for at least 24 months on ART (**a**) and in 15 viremic patients (median CD4 T-cell count = 477 per mm³, median viral load = 3.3 log₁₀, **b**). Data are expressed as the difference in PD-1 mean fluorescence intensity (Δ MFI) relative to naive CD4⁺ T cells. Boxes represent the median and the 25th and 75th percentiles; whiskers represent the 10th and 90th percentiles. Representative PD-1 staining is shown. The data were analysed with the Friedman test for paired data and with Dunn's multiple comparison test (* $P < 0.05$, ** $P < 0.01$, *** $P < 0.001$, **** $P < 0.0001$).

compared with other CD4 memory subsets in viremic patients and patients on ART with undetectable plasma virus. This was consistent with previous reports suggesting that in CD4 and CD8 T cells the expression of the inhibitory receptor PD-1 could be related to the stage of differentiation^{5,19,20}. PD-1 could represent a potential target to facilitate HIV eradication^{5,21}. However, the low PD-1 expression on T_{SCM} argues against an effectiveness of PD-1 targeting therapies in reducing the size of the T_{SCM} sub-reservoir. Alternatively, the presence within a memory subset of latently infected cells generated by indirect infection, for example, through cell transfer from the T_{SCM} pool towards more highly differentiated memory subsets, might also alter the direct relationship between the size of the sub-reservoir and cumulative viral exposure.

Our results show that it is unrealistic to expect ART alone to purge the latent HIV reservoir. PCR procedures for detecting integrated HIV may overestimate the size of the latent CD4⁺ T-cell reservoir. Indeed, a significant proportion of integrated viruses is assumed to be defective because it cannot be induced by *in vitro* activation. Importantly, the stimuli used *in vitro* to activate cells and to recover latent virus in outgrowth assays may not fully reproduce the complex activation conditions existing *in vivo*, particularly given the marked immunological heterogeneity of the latent reservoir cells. Indeed, this reservoir comprises different CD4⁺ T-cell subsets with distinct activation requirements (for instance, see Fig. 4a,b, showing variable expression of the inhibitory receptor PD-1 by different cell subsets). This implies that some latent viruses capable of generating infective virions *in vivo* may not be recoverable *in vitro*. Also, a recent elegant study showed that the latent reservoir contains proviruses with no deletions or inactivating mutations that are not induced after *in vitro* activation, but might possibly be recoverable *in vivo*²². The authors of this latter study forwarded a model of stochastic induction of intact proviruses following cell activation²². Clearly, although PCR procedures for

detecting integrated HIV may overestimate the size of the latent reservoir, viral outgrowth assays can underestimate it²². In practice, this means that a patient cannot be said to be cured of HIV infection unless integrated virus is undetectable by PCR.

The part of the latent CD4 T-cell reservoir formed by T_{CM} and T_{SCM} should be a priority target for therapeutic strategies addressing the latent reservoir. Therapeutic approaches targeting key memory and effector differentiation pathways could also help to drive latently infected memory cells, beyond the effector memory state, towards short-lived terminally differentiated effector states, thereby accelerating the decay of the latent reservoir. Our results also stress the importance of early initiation of effective ART to limit the size of the T_{SCM} reservoir, which appears directly related to cumulative plasma virus exposure.

Methods

Patients. Patients were selected from a cohort of 360 HIV-1-infected patients in whom plasma viral load was determined every 3 months. To be eligible for the study, patients had to have undetectable plasma virus on combined antiretroviral therapy (ART) for at least 24 months. Detection of a single viral blip was a formal exclusion criterion. Patients also had to have a CD4⁺ T-cell count higher than 500 per mm³ of blood, indicating effective immune recovery on ART, at the time when their cell subsets were tested for integrated HIV or for viral production. Forty-five eligible patients (plasma virus load undetectable (<20 copies per ml) for 24–189 months) agreed to participate in this cross-sectional study. Integrated HIV DNA was quantified in 38 patients. Characteristics of the patients are indicated in Supplementary Table 1. Cells from seven patients with undetectable plasma virus for 34–148 months were used for inducing virus production *in vitro*. Written informed consent was obtained from each patient and the study was approved by the local ethics committee (Comité pour la Protection des Personnes Ile-de-France VII, (CPP IDF VII) Bicêtre, France). Cumulative HIV plasma viremia up to the time when plasma virus became undetectable (from 12–84 months before than plasma virus became undetectable) was determined as previously described¹³ in patients for whom plasma viral load data were available.

Flow cytometry. A blood sample of 200 μ l was used for CD4⁺ memory T-cell phenotyping with the following antibodies: anti-CD8-FITC (1/10, clone RPA-T8), anti-PD1-FITC (1/5, clone MIH4), anti-CD122-PE (1/10, clone Mik-B3),

anti-CD62L-V450 (1/10, clone DREG-56), anti-CD4-V500 (1/20, clone RPA-T4), anti-CD95-APC (1/10, clone DX2), anti-CD45RA-PE-Cy7 (1/20, clone HI100), anti-CD45RO-PerCP-Cy5.5 (1/10, clone UCHL1), anti-CCR7-PE-CF594 (1/10, clone 150503), anti-CXCR3-Alexa 700 (1/10, clone 1C6/CXCR3), anti-CD27-APC-H7 (1/10, clone M-T271) (all from BD Biosciences), and anti-CD3-eFluor 650NC (1/10, clone OKT3, eBioscience). After staining, the blood sample was fixed (fix/lyse solution, BD Biosciences) and cells were acquired on a BD LSR Fortessa cytometer (BD Biosciences). Data were analysed with Flow Jo software.

Cell sorting. CD4⁺ T cells were enriched from PBMC by negative selection with magnetic beads (CD4 BD Imag, BD Biosciences). The cells were then stained with a cocktail of the following antibodies: anti-HLA-DR-FITC (1/15, clone G4-6), anti-CD8 FITC (1/15, clone RPA-T8), anti-CD19-FITC (1/15, clone HIB19), anti-CD14 FITC (1/15, clone M5E2), anti-CD25-FITC (1/6, clone M-A251), anti-CD69-FITC (1/6, clone FN50), anti-CD3-Alexa 700 (1/15, clone OKT3), anti-CD122-PE (1/12, clone Mik-B3), anti-CD62L-V450 (1/15, clone DREG-56), anti-CD4-V500 (1/30, clone RPA-T4), anti-CD95-APC (1/15, clone DX2), anti-CD45RA-PE-Cy7 (1/30, clone HI100), anti-CD45RO-PerCP-Cy5.5 (1/15, clone UCHL1), anti-CCR7-PE-CF594 (1/15, clone 150503) and anti-CD27-APC-H7 (1/30, clone M-T271) (all from BD Biosciences), then sorted with a BD Facs ARIA III cytometer (BD Biosciences). Non-CD4⁺ T cells and possibly activated CD4⁺ T cells were gated out by fluorescein isothiocyanate staining. After gating on the live-cell gate and doublet exclusion, highly purified memory CD4⁺ T-cell subsets were sorted on the basis of the following phenotypes: (i) stem cell memory CD4⁺ T cells (T_{SCM}): CD3⁺ CD4⁺ CD45RA⁺ CD45RO⁻ CCR7⁺ CD62L⁺ CD27⁺ CD95⁺⁹; (ii) central memory CD4⁺ T cells (T_{CM}): CD3⁺ CD4⁺ CD45RA⁻ CD45RO⁺ CCR7⁺ CD62L⁺ and (iii) effector memory CD4 T cells (T_{EM}): CD3⁺ CD4⁺ CD45RA⁻ CD45RO⁺ CCR7⁻ CD62L⁻. An additional subset with an intermediate phenotype (T_{IM}) was also sorted: CD3⁺ CD4⁺ CD45RA⁻ CD45RO⁺ CCR7⁻ CD62L⁺.

Latent HIV quantification. Integrated HIV DNA was quantified by two-step ALU-gag PCR as previously described^{10,11} (see also Supplementary Fig. 6). Serial dilutions of the 8E5 cell line (American Type Culture Collection) in PBMC from HIV-seronegative donors were used to generate a standard curve with which to quantify integrated HIV DNA (Supplementary Fig. 6a). The 8E5 cell line harbours a single integrated HIV copy per genome. The standard curve spanned 2,000 to 1 HIV copies per PCR. The PCR method was able to detect one integrated HIV DNA copy (one 8E5 cell) among 100,000 cellular genomes (Supplementary Fig. 6a). The same numbers of resting T_{SCM}, T_{CM}, T_{EM} and T_{IM}, corresponding to the lowest cell number recovered among the four cell subsets after sorting, were pelleted for DNA extraction. In all patients, glyceraldehyde 3-phosphate dehydrogenase quantitative PCR performed on 10% of the extracted DNA showed that similar amounts of DNA were effectively recovered from the cell subsets. Duplicate cell aliquots were used whenever possible. The product of the first Alu-gag PCR was split into five 10-μl aliquots, and each aliquot was submitted to nested PCR^{10,11}. We used the mean value obtained for the five aliquots. When duplicate cellular aliquots were available, we used the mean of the ten values. Additional information about Latent HIV quantification is provided in Supplementary Methods.

Statistical analysis. Statistical analysis was performed using Prism software (GraphPad). Differences between groups were analysed using the Kruskal–Wallis and Dunn's tests for unpaired continuous variables, and the Friedman and Dunn tests for paired continuous variables. The χ^2 test was used for categorical variables. The Spearman rank test was used to examine associations between the size of the latently infected memory subsets at the time when plasma virus became undetectable and parameters including age and sex, the CD4⁺ T-cell nadir, the duration of HIV viremia and cumulative HIV viremia before plasma virus becoming undetectable.

Estimation of decay rates of CD4⁺ T-cell sub-reservoirs. Bootstrapping is a statistic method for assigning measures of accuracy to estimates^{23,24}. A standard choice for approximating the distribution is to use the empirical distribution of the observed data. This can be implemented by constructing a number of resamples of the data set, each of which is obtained by random sampling with replacement from the original data set.

In this paper, for each CD4⁺ T-cell memory reservoir, we consider the following model:

$$y = y_0 e^{\lambda t} \quad (1)$$

where y_0 is the integrated HIV DNA copy number at the time of undetectable plasma virus following ART initiation, λ is the slope of decay for each latent sub-reservoir and t is the duration of plasma virus undetectability. The half-life is computed with the term $-\ln 2/\lambda$. Note that we considered nonlinear mathematical models, however we could not find any statistically significant improvement.

Therefore, given a vector observation (measurement) y_i at time t_i , the parameter set $\phi = [\lambda, y_0]$ is computed for each CD4⁺ T-cell memory sub-reservoir (inverse problem²⁵).

The parameter fitting is performed by minimizing the root mean square difference on a *log* scale between the model predictive output (x_i) and the experimental measurement (y_i), as follows:

$$RMS = \sqrt{\frac{1}{n} \sum_{i=1}^n (\log(y_i) - \log(x_i))^2} \quad (2)$$

where n is the total number of measurements. The minimization of root mean square is performed using the differential evolution algorithm²⁵. Several optimization solvers were tested, including both deterministic (fmincon Matlab routine, Threshold Acceptance algorithm and Pattern Search algorithm) and stochastic methods (Genetic algorithm and Annealing algorithm). We found that the differential evolution global optimization algorithm was robust to initial guesses of parameters and converged faster with more certainty than the other methods.

As inter-patient variability is non-negligible in this work, we considered the bootstrap method to analyse mathematical models in stochastic environments. Bootstrap is useful when there is no form to estimate the distribution of the statistic of interest²⁴. One way of performing case resampling is to use the MC algorithm. This methodology has been successfully used to address different biological problems^{24,26}.

MC Analysis. The MC algorithm^{24,27} is a large dimensional-space method that uses repeated random samplings to obtain numerical results in a stochastic environment when experiments cannot be repeated several times and when variability is present.

To settle down the simulations, we resample the data with replacements. The size of the resample must be equal to the size of the original set. To this end, based on the variance of our raw data for each time point in Fig. 2a, we generated a vector with random samplings using a geometric distribution (results were consistent using normal or exponential distribution). Using equation (1), we again refitted the parameters (λ , y_0), and repeated this process 10⁶ times for each CD4⁺ T-cell subset. This large number of repetitions provides a more precise estimate of the parameter distribution. Histograms showing the distribution of y_0 and λ obtained by bootstrapping can be found in Supplementary Fig. 8. The 95% confidence interval of parameter estimates is computed using the outcome of the bootstrap method²⁸. For each constant parameter, we select the 2.5 and 97.5% quantiles of the 10⁶ estimates to form the 95% confidence interval. The results are presented in Supplementary Fig. 8.

Analyses of the MC outcome were implemented with two-way analysis of variance and a *t*-test. Significance was assumed at $P < 0.05$, and the data were further analysed with a Bonferroni post-test.

References

- Chun, T. W. *et al.* Quantification of latent tissue reservoirs and total body viral load in HIV-1 infection. *Nature* **387**, 183–188 (1997).
- Chun, T. W. *et al.* Presence of an inducible HIV-1 latent reservoir during highly active antiretroviral therapy. *Proc. Natl Acad. Sci. USA* **94**, 13193–13197 (1997).
- Finzi, D. *et al.* Latent infection of CD4⁺ T cells provides a mechanism for lifelong persistence of HIV-1, even in patients on effective combination therapy. *Nat. Med.* **5**, 512–517 (1999).
- Finzi, D. *et al.* Identification of a reservoir for HIV-1 in patients on highly active antiretroviral therapy. *Science (New York, NY)* **278**, 1295–1300 (1997).
- Chomont, N. *et al.* HIV reservoir size and persistence are driven by T cell survival and homeostatic proliferation. *Nat. Med.* **15**, 893–900 (2009).
- Tran, T. A. *et al.* Resting regulatory CD4 T cells: a site of HIV persistence in patients on long-term effective antiretroviral therapy. *PLoS ONE* **3**, e3305 (2008).
- Costantini, A. *et al.* Effects of cryopreservation on lymphocyte immunophenotype and function. *J. Immunol. Methods* **278**, 145–155 (2003).
- Weinberg, A. *et al.* Optimization and limitations of use of cryopreserved peripheral blood mononuclear cells for functional and phenotypic T-cell characterization. *Clin. Vaccine Immunol.* **16**, 1176–1186 (2009).
- Gattinoni, L. *et al.* A human memory T cell subset with stem cell-like properties. *Nat. Med.* **17**, 1290–1297 (2011).
- Liszewski, M. K., Yu, J. J. & O'Doherty, U. Detecting HIV-1 integration by repetitive-sampling Alu-gag PCR. *Methods (San Diego, Calif)* **47**, 254–260 (2009).
- Yu, J. J. *et al.* A more precise HIV integration assay designed to detect small differences finds lower levels of integrated DNA in HAART treated patients. *Virology* **379**, 78–86 (2008).
- Cole, S. R. *et al.* Copy-years viremia as a measure of cumulative human immunodeficiency virus viral burden. *Am. J. Epidemiol.* **171**, 198–205 (2010).
- Kim, H. & Perelson, A. S. Viral and latent reservoir persistence in HIV-1-infected patients on therapy. *PLoS Comput. Biol.* **2**, e135 (2006).

14. Vandergeeten, C. *et al.* Interleukin-7 promotes HIV persistence during antiretroviral therapy. *Blood* **121**, 4321–4329 (2013).
15. Lugli, E. *et al.* Superior T memory stem cell persistence supports long-lived T cell memory. *J. Clin. Invest.* **123**, 594–599 (2013).
16. Buzon, M. J. *et al.* HIV-1 persistence in CD4 T cells with stem cell-like properties. *Nat. Med.* **20**, 139–142 (2014).
17. Mexas, A. M. *et al.* Concurrent measures of total and integrated HIV DNA monitor reservoirs and ongoing replication in eradication trials. *AIDS (London, England)* **26**, 2295–2306 (2012).
18. Agosto, L. M. *et al.* Patients on HAART often have an excess of unintegrated HIV DNA: implications for monitoring reservoirs. *Virology* **409**, 46–53 (2011).
19. Adekambi, T. *et al.* Distinct effector memory CD4⁺ T cell signatures in latent *Mycobacterium tuberculosis* infection, BCG vaccination and clinically resolved tuberculosis. *PLoS ONE* **7**, e36046 (2012).
20. Sauce, D. *et al.* PD-1 expression on human CD8 T cells depends on both state of differentiation and activation status. *AIDS (London, England)* **21**, 2005–2013 (2007).
21. Porichis, F. & Kaufmann, D. E. Role of PD-1 in HIV pathogenesis and as target for therapy. *Curr. HIV/AIDS Rep.* **9**, 81–90 (2012).
22. Ho, Y. C. *et al.* Replication-competent noninduced proviruses in the latent reservoir increase barrier to HIV-1 cure. *Cell* **155**, 540–551 (2013).
23. Chernick, M. R. *Bootstrap Methods: A Practitioner's Guide* (Wiley, 1999).
24. Davison, A. C. & Hinkley, D. V. *Bootstrap Methods and Their Application* (Cambridge Univ., 1997).
25. Storn, R. & Price, K. Differential evolution a simple and efficient heuristic for global optimization over continuous spaces. *J. Global Optim.* **11**, 341–359 (1997).
26. Hernandez-Vargas, E. A. *et al.* The effects of aging on influenza virus infection dynamics. *J. Virol.* **88**, 4123–4131 (2014).
27. Anderson, H. L. Metropolis, Monte Carlo and the MANIAC. *Los Alamos Science* **14**, 96–108 (1986).
28. Xue, H., Miao, H. & Wu, H. Sieve estimation of constant and time varying coefficients in nonlinear ordinary differential equation models by considering both numerical error and measurement error. *Ann. Stat.* **38**, 2351–2387 (2010).
29. Cameron, J. R., Skofronick, J. G. & Grant, R. M. *Physics of the Body* 2nd edn (Medical Physics Publishing, 1999).

Acknowledgements

This work was supported by ANRS (Agence Nationale de Recherche sur le SIDA, 75013 Paris, France). S.J. has a fellowship grant from ANRS. We thank K Bourdic, M Mole, MJ Dulucq and all the nurses at the HIV Daycare Unit, Department of Internal Medicine, Bicêtre Hospital, 94276 le Kremlin-Bicêtre, France.

Author contributions

S.J. designed and performed experiments and analysed data. M.G.deG.deH. designed and performed experiments, analysed data, performed statistical analysis and wrote the paper. E.A.H.-V. analysed data, performed mathematical modelling and statistical analysis and wrote the paper. M.A. performed experiments and analysed data. M.C.M. performed experiments and analysed data. R.K. analysed data. M.M. selected patients and analysed data. R.S. performed statistical analysis. M.T. designed experiments and analysed data. J.F.D. designed experiments and analysed data. C.G. selected patients, designed experiments and analysed results. Y.T. designed experiments, analysed data, wrote the paper and supervised the project.

Additional information

Supplementary Information accompanies this paper at <http://www.nature.com/naturecommunications>

Competing financial interests: The authors declare no competing financial interests.

Reprints and permission information is available online at <http://npg.nature.com/reprintsandpermissions/>

How to cite this article: Jaafoura, S. *et al.* Progressive contraction of the latent HIV reservoir around a core of less-differentiated CD4⁺ memory T-Cells. *Nat. Commun.* **5**:5407 doi: 10.1038/ncomms6407 (2014).



This work is licensed under a Creative Commons Attribution 4.0 International License. The images or other third party material in this article are included in the article's Creative Commons license, unless indicated otherwise in the credit line; if the material is not included under the Creative Commons license, users will need to obtain permission from the license holder to reproduce the material. To view a copy of this license, visit <http://creativecommons.org/licenses/by/4.0/>